Pergamon

0045-7949(95)00017-8

Computers & Structures Vol. 56, No. 2/3, pp. 225–237, 1995

0045-7949/95 $9.50 + 0.00

A MIXED DISPLACEMENT-BASED FINITE ELEMENT FORMULATION FOR ACOUSTIC FLUID–STRUCTURE INTERACTION

K. J. Bathe, C. Nitikitpaiboon and **X. Wang**
Massachusetts Institute of Technology, Cambridge, MA 02139, U.S.A.

Abstract—The solutions of fluid–structure interaction problems, using displacement-based finite element formulations for acoustic fluids, may contain spurious non-zero frequencies. To remove this deficiency, we present here a new formulation based on a three-field discretization using displacements, pressure and a "vorticity moment" as variables with an appropriate treatment of the boundary conditions. We propose specific finite element discretizations and give the numerical results of various example problems.

1. INTRODUCTION

The interaction between fluids and structures can, in many practical engineering analyses, significantly affect the response of the structure and hence needs to be taken into account properly. As a result, much effort has gone into the development of general finite element methods for fluid–structure systems.

A number of finite element formulations have been proposed for acoustic fluids in the analysis of fluid–structure interaction problems, namely, the displacement formulation (see Hamdi *et al.* [1], Belytschko and Kennedy [2], Belytschko [3], Olson and Bathe [4]), the displacement potential and pressure formulation (Morand and Ohayon [5]), and the velocity potential formulation (Everstine [6], Olson and Bathe [7]). The displacement formulation has received considerable attention, because it does not require any special interface conditions or new solution strategies (for example, in frequency calculations and response spectrum analyses) and because of the potential applicability to the solution of a broad range of problems.

It has been widely recognized that the displacement-based fluid elements employed in frequency or dynamic analyses exhibit spurious *non-zero* circulation modes. Various approaches have been introduced to obtain improved formulations. The penalty method has been applied by Hamdi *et al.* [1] and has been shown to give good solutions for the cases considered in that reference. Subsequently, Olson and Bathe [4] demonstrated that the method "locks up" in the frequency analysis of a solid vibrating in a fluid cavity and that reduced integration performed on the penalty formulation yields some improvement in results but does not assure solution convergence in a general case. More recently, Chen and Taylor proposed a four-node element based on a reduced integration technique together with an element mass matrix projection [8]. The element is used to solve some example problems, but an analysis or numerical results on whether the element formulation is stable and reliable are not presented.

Therefore, although much research has been expended on the topic, we believe that the currently available displacement-based formulations of fluids and fluid–structure interactions are not yet satisfactory.

Our objective in this study was to develop a formulation to overcome the aforementioned difficulties. Since mixed methods are now used with considerable success for other types of constraint problems, we endeavored to develop a displacement-based mixed finite element formulation for the fluid. As reported in this paper, we arrived at a three-field mixed variational principle and new fluid elements which yield very promising results.

In the following sections we first summarize the assumptions and governing equations used in our mathematical model. Next, we discuss the difficulties present in the ordinary displacement formulation. Finally, the new three-field displacement-pressure-vorticity moment ($\mathbf{u}$–p–$\boldsymbol{\Lambda}$) formulation is presented in detail with some solution results.

2. GOVERNING EQUATIONS

Our objective is to evaluate the lowest frequencies of fluid–structure systems. We assume an inviscid isentropic fluid undergoing small vibrations for which the governing equations in the fluid domain $\mathbf{V}_f$ are

$$\rho\dot{\mathbf{v}} + \nabla p = \mathbf{0} \tag{1}$$

$$\beta\nabla\cdot\mathbf{v} + \dot{p} = 0 \tag{2}$$

where $\mathbf{v}$ is the velocity vector, p is the pressure, ρ is the mass density and the bulk modulus, β, can be

written in terms of the sound wave speed, c, as

$$\beta = \rho c^2. \tag{3}$$

The boundary conditions are that $\bar{p}$ is the prescribed pressure on the surface S_f and $\bar{u}_n$ is the prescribed normal displacement on the surface S_u, with the unit normal vector $\mathbf{n}$ pointing outward from the fluid domain. Also, we have $S_u \cup S_f = S$ and $S_u \cap S_f = \varnothing$.

We note that eqn (2) implies

$$\nabla \cdot \mathbf{u} = -\frac{p}{\beta} \tag{4}$$

where $\mathbf{u}$ is the displacement vector. Therefore, when almost incompressible conditions are considered, (that is, when β is large while p is of the order of the stress and hence relatively small) we have that $\nabla \cdot \mathbf{u}$ is close to zero. Also, eqn (1) implies

$$\frac{\partial}{\partial t}(\nabla \times \mathbf{v}) = \mathbf{0} \tag{5}$$

and hence the motion is always circulation preserving, i.e. it is a motion in which the vorticity does not change with time.

In terms of the displacements only, we have by substituting from eqn (4) into eqn (1)

$$\beta \nabla(\nabla \cdot \mathbf{u}) + \mathbf{f}^B = \mathbf{0} \tag{6}$$

where $\mathbf{f}^B = -\rho \ddot{\mathbf{u}}$. Hence $\mathbf{f}^B$ is a vector of body forces per unit volume which we assume to contain only the inertia forces, but other contributions could directly be included.

In the frequency solution, the governing equation is

$$c^2 \nabla(\nabla \cdot \tilde{\mathbf{U}}) + \omega^2 \tilde{\mathbf{U}} = \mathbf{0} \tag{7}$$

where $\tilde{\mathbf{U}}$ represents the eigenfunction. It then follows that

$$\beta \nabla \times (\nabla(\nabla \cdot \tilde{\mathbf{U}})) + \rho \omega^2 (\nabla \times \tilde{\mathbf{U}}) = \mathbf{0}. \tag{8}$$

Since $\nabla \times \nabla \phi = \mathbf{0}$ for any smooth scalar valued function ϕ, we have that

$$\omega^2 (\nabla \times \tilde{\mathbf{U}}) = \mathbf{0} \tag{9}$$

It is then apparent that in a frequency analysis the system admits two types of analytical solutions; namely, solutions corresponding to the rotational motions ($\nabla \times \tilde{\mathbf{U}} \neq \mathbf{0}$) for which the frequencies are zero, and solutions corresponding to the irrotational motions ($\nabla \times \tilde{\mathbf{U}} = \mathbf{0}$). One may view the first type of solution as the way the system responds to the rotational initial boundary conditions.

The variational form of eqn (6) is given by

$$\int_{V_f} \{\beta(\nabla \cdot \mathbf{u})(\nabla \cdot \delta \mathbf{u}) - \mathbf{f}^B \cdot \delta \mathbf{u}\} \, \mathrm{d}V + \int_{S_f} \bar{p} \delta u_n^S \, \mathrm{d}S = 0 \tag{10}$$

where u_n^S is the displacement normal to S_f. The variational indicator is

$$\Pi = \int_{V_f} \left\{ \frac{\beta}{2} (\nabla \cdot \mathbf{u})^2 - \mathbf{f}^B \cdot \mathbf{u} \right\} \mathrm{d}V + \int_{S_f} \bar{p} u_n^S \, \mathrm{d}S. \tag{11}$$

This variational indicator is used for the ordinary displacement-based finite element discretization of acoustic fluids. It has been observed that *a finite element solution based on eqn (11) may yield, other than the zero frequency circulation modes, also circulation modes with non-zero frequencies.* While the circulation modes with zero frequencies can easily be recognized and discarded in a dynamic solution, that is, a mode superposition solution, spurious non-zero frequencies are difficult to identify in practice and should not be present in a reliable finite element analysis.

In order to eliminate the spurious non-zero frequencies, we impose the constraint

$$\nabla \times \mathbf{u} = \frac{\boldsymbol{\Lambda}}{\alpha} \tag{12}$$

where $\boldsymbol{\Lambda}$ is a "vorticity moment". The magnitude of $\boldsymbol{\Lambda}$ shall be small while α is a constant of large value.

In addition, when the fluid acts in almost incompressible conditions, we have the usual constraint of near incompressibility, see eqn (4). As demonstrated by Olson and Bathe, a pure displacement formulation with the two constraints of irrotationality and (almost) incompressibility yields much too stiff response predictions, typical of the "locking" behavior [4].

However, we now recall our experiences with the displacement/pressure formulation for solids (or velocity/pressure formulation for viscous fluids) which, with the proper choice of elements, is very effective in almost incompressible situations [9]. These experiences lead us to propose a displacement-based mixed formulation which properly incorporates the above two constraints and provides excellent promise for general applications.

3. VARIATIONAL FORMULATION

Based on our experience with the displacement (velocity)/pressure formulation for (almost) incompressible media, we propose the following variational indicator for the finite element formulation of the

fluid considered here:

$$\Pi = \int_{V_f} \left\{ \frac{p^2}{2\beta} - \mathbf{u}\cdot\mathbf{f}^B - \lambda_p\left(\frac{p}{\beta} + \nabla\cdot\mathbf{u}\right) + \frac{\boldsymbol{\Lambda}\cdot\boldsymbol{\Lambda}}{2\alpha} - \boldsymbol{\lambda}_\Lambda\cdot\left(\frac{\boldsymbol{\Lambda}}{\alpha} - \nabla\times\mathbf{u}\right)\right\} dV + \int_{S_f} \bar{p}u_n^S\, dS \tag{13}$$

where the variables are the pressure p, displacement $\mathbf{u}$, vorticity moment $\boldsymbol{\Lambda}$, and the Lagrange multipliers λ_p and $\boldsymbol{\lambda}_\Lambda$. The constant β is the bulk modulus and the constant α have large values. We note that the first two terms correspond to the usual strain energy (given in terms of the pressure) and the potential of the externally applied body forces. The third term implies the constraint in eqn (4), the fourth term is included to be able to statically condense out the degrees of freedom of the vorticity moment and the fifth term imposes the constraint in eqn (12). For the fourth and fifth terms we require that the constant α is large, and we use $\alpha = 1000\beta$. However, from our numerical tests, we find that α can be any numerically reasonable value larger than β, say $10\beta \leqslant \alpha \leqslant 10^4\beta$.

The last term is the potential due to any applied boundary pressure on the surface S_f.

Invoking the stationarity of Π, we identify the Lagrange multipliers λ_p and $\boldsymbol{\lambda}_\Lambda$ to be the pressure p and vorticity moment $\boldsymbol{\Lambda}$, respectively, and we obtain the field equations

$$\nabla p - \mathbf{f}^B + \nabla\times\boldsymbol{\Lambda} = \mathbf{0} \tag{14}$$

$$\nabla\cdot\mathbf{u} + \frac{p}{\beta} = 0 \tag{15}$$

$$\nabla\times\mathbf{u} - \frac{\boldsymbol{\Lambda}}{\alpha} = \mathbf{0} \tag{16}$$

and the boundary conditions

$$\mathbf{u}\cdot\mathbf{n} = \bar{u}_n \quad \text{on } S_u$$

$$p = \bar{p} \quad \text{on } S_f$$

$$\boldsymbol{\Lambda} = \mathbf{0} \quad \text{on } S. \tag{17}$$

The pressure $\bar{p}$ is commonly assigned to be zero on the free surface. Also, in the variational indicator, ignoring gravity effects and other body forces, we have $\mathbf{f}^B = -\rho\ddot{\mathbf{u}}$.

4. FINITE ELEMENT DISCRETIZATION

We use the standard procedure of finite element discretization [9] and hence for a typical element, we have

$$\mathbf{u} = \mathbf{H}\hat{\mathbf{U}}$$

$$p = \mathbf{H}_p\hat{\mathbf{P}}$$

$$\boldsymbol{\Lambda} = \mathbf{H}_\Lambda\hat{\boldsymbol{\Lambda}}$$

$$\nabla\cdot\mathbf{u} = (\nabla\cdot\mathbf{H})\hat{\mathbf{U}} = \mathbf{B}\hat{\mathbf{U}}$$

$$\nabla\times\mathbf{u} = (\nabla\times\mathbf{H})\hat{\mathbf{U}} = \mathbf{D}\hat{\mathbf{U}}$$

where $\mathbf{H}$, $\mathbf{H}_p$ and $\mathbf{H}_\Lambda$ are the interpolation matrices, and $\hat{\mathbf{U}}$, $\hat{\mathbf{P}}$ and $\hat{\boldsymbol{\Lambda}}$ are the vectors of solution variables.

The matrix equations of our formulation are

$$\begin{bmatrix} \mathbf{M} & \mathbf{0} & \mathbf{0} \\ \mathbf{0} & \mathbf{0} & \mathbf{0} \\ \mathbf{0} & \mathbf{0} & \mathbf{0} \end{bmatrix} \begin{Bmatrix} \ddot{\hat{\mathbf{U}}} \\ \ddot{\hat{\mathbf{P}}} \\ \ddot{\hat{\boldsymbol{\Lambda}}} \end{Bmatrix} + \begin{bmatrix} \mathbf{0} & \mathbf{L} & \mathbf{Q} \\ \mathbf{L}^T & \mathbf{A} & \mathbf{0} \\ \mathbf{Q}^T & \mathbf{0} & \mathbf{G} \end{bmatrix} \begin{Bmatrix} \hat{\mathbf{U}} \\ \hat{\mathbf{P}} \\ \hat{\boldsymbol{\Lambda}} \end{Bmatrix} = \begin{Bmatrix} \mathbf{R} \\ \mathbf{0} \\ \mathbf{0} \end{Bmatrix} \tag{18}$$

where

$$\mathbf{M} = \int_{V_f} \rho\mathbf{H}^T\mathbf{H}\, dV \qquad \mathbf{L} = -\int_{V_f} \mathbf{B}^T\mathbf{H}_p\, dV$$

$$\mathbf{Q} = \int_{V_f} \mathbf{D}^T\mathbf{H}_\Lambda\, dV \qquad \mathbf{A} = -\int_{V_f} \frac{1}{\beta}\mathbf{H}_p^T\mathbf{H}_p\, dV$$

$$\mathbf{G} = -\int_{V_f} \frac{1}{\alpha}\mathbf{H}_\Lambda^T\mathbf{H}_\Lambda\, dV \qquad \mathbf{R} = -\int_{S_f} \mathbf{H}_n^{S^T}\bar{p}\, dS. \tag{19}$$

The key to the success of the finite element discretization is to choose the appropriate interpolations for the displacements, pressure and vorticity moment. Without restricting the essence of our exposition, let us consider two-dimensional solutions. The finite element formulation for three-dimensional solutions is then directly obtained [9].

Considering (almost) incompressible analysis of solids and viscous fluids, it is well-established that finite elements which satisfy the inf-sup condition are effective and reliable. Appropriate interpolations are summarized in Refs [9], [10] and [11]. The u/p elements give continuous displacements (or velocities) and discontinuous pressures whereas the u/p-c elements yield continuous displacements (or velocities) and pressures across the element boundaries.

For the inviscid fluid element formulation considered here, we use the displacement/pressure interpolations that satisfy the inf-sup condition in the analysis of solids (and viscid fluids) and use the same interpolation for the vorticity moment as for the pressure. Thus, two proposed elements are the 9-3-3 and 9-4c-4c elements schematically depicted in Fig. 1.

Hence, for the 9-3-3 element, we interpolate the pressure and vorticity moment linearly as

$$p = p_1 + p_2 r + p_3 s \tag{20}$$

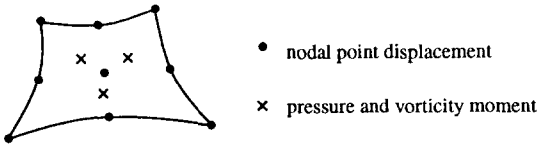

9-3-3 element

continuous displacement, discontinuous pressure and vorticity moment

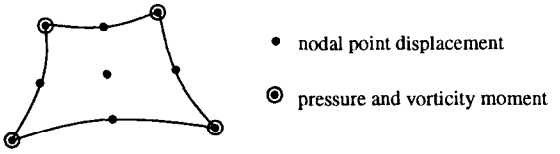

9-4c-4c element

continuous displacement, pressure and vorticity moment

Fig. 1. Two elements for $\mathbf{u}$–p–Λ formulation. Full numerical integration is used (i.e. 3 × 3 Gauss integration).

$$\Lambda = \Lambda_1 + \Lambda_2 r + \Lambda_3 s \tag{21}$$

and for the 9-4c-4c element we use the bilinear interpolations

$$p = p_1 + p_2 r + p_3 s + p_4 rs \tag{22}$$

$$\Lambda = \Lambda_1 + \Lambda_2 r + \Lambda_3 s + \Lambda_4 rs. \tag{23}$$

Of course, additional elements could be proposed using this approach. In each case, the vorticity moment would be interpolated with functions that when used for the pressure interpolation give a stable element for (almost) incompressible conditions. For instance, a reasonable element is also the 9-3-1 element, which however does not impose the zero vorticity as strongly as the 9-3-3 element. On the other hand, the 4-1-1 element cannot be recommended (see Section 6 for some numerical results obtained with this element). For all elements full numerical integration is used [9].

While we do not have a mathematical analysis to prove that the proposed elements are indeed stable, based on our experience we can expect a good element behavior. Namely, the constraints in eqn (4) and (12) are very similar in nature and are not coupled in the formulation, see the variational indicator in eqn (13). Hence, we can reasonably assume that the two constraints should be imposed with the same interpolations in the element discretization.

5. BOUNARY CONDITIONS

The above finite element formulation appears to be rather natural, when considering the literature available on elements that perform well in incompressible analysis of solids (or viscous fluids). However, some subtle points arise in imposing the boundary conditions.

Let us consider typical boundary lines composed of two adjacent three or four-node elements, see Fig. 2, and two nine-node elements, see Fig. 3. Since the fluid is inviscid, the displacement component tangential to the solid is not restrained (while the displacement component normal to the solid is restrained to be equal to the displacement of the solid). The choice of directions of nodal tangential displacements (from which also follow the directions for the normal displacements) is critical.

Considering the solution of actual fluid flows and fluid flows with structural interactions (in which the fluid is modeled using the Navier–Stokes equations including wall turbulence effects or the Euler equations), we are accustomed to choosing these directions such that in the finite element discretization there is no transport of fluid across the fluid boundary. It is important that we employ the same concept also in the definition of the tangential directions at boundary nodes of the acoustic fluid considered here, although the acoustic fluid does not flow but only undergoes (infinitesimally) small displacements.

While we do not recommend using the 4-1-1 element of our $\mathbf{u}$–p–Λ formulation (see Table 4 and Figs 15 and 16), lower-order elements (three-node triangular two-dimensional and four-node tetrahedral three-dimensional elements with bubble functions) are effectively employed in fluid flow analysis and could be used in our $\mathbf{u}$–p–Λ formulation [9, 12].

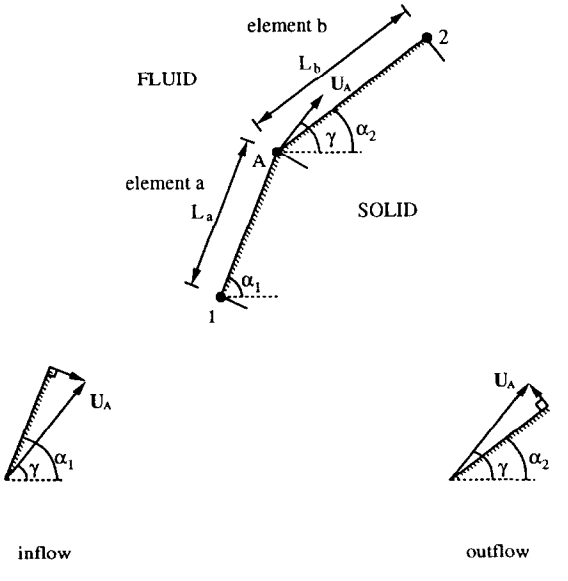

Fig. 2. Tangential direction given by γ at node A for 3 or 4-node elements.

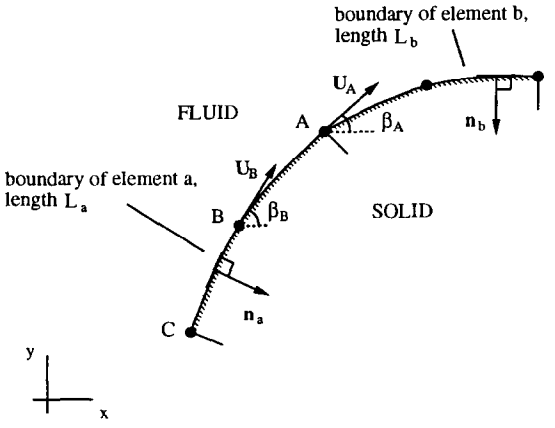

Fig. 3. Tangential directions given by β_A and β_B at nodes A and B for 9-node elements.

Hence consider first the boundary representation in Fig. 2. This case was already discussed by Donea *et al.* [13]. For the displacement $\mathbf{U}_A$, we have the spurious fluxes ΔV_a and ΔV_b across the element lengths L_a and L_b. Mass conservation requires that $\Delta V_a + \Delta V_b = 0$ and hence we must choose γ given by

$$\tan\gamma = \frac{L_a \sin\alpha_1 + L_b \sin\alpha_2}{L_a \cos\alpha_1 + L_b \cos\alpha_2}. \tag{24}$$

We note that γ is actually given by the direction of the line from node one to node two. In general, the direction of $\mathbf{U}_A$ is not given by the mean of the angles α_1 and α_2, but only in the specific case when $L_a = L_b$

$$\gamma = \tfrac{1}{2}(\alpha_1 + \alpha_2). \tag{25}$$

We employ the same concept to establish the appropriate tangential directions at the typical nodes A and B of our nine-node elements in Fig. 3. For node A, we need to have using β_A

$$\int_{L_a} \mathbf{u}_a^A \cdot \mathbf{n}_a \, dl + \int_{L_b} \mathbf{u}_b^A \cdot \mathbf{n}_b \, dl = 0 \tag{26}$$

where

$$\mathbf{n}_a \, dl = \left(-\frac{\partial y_a}{\partial s} ds, \frac{\partial x_a}{\partial s} ds \right)$$

$$\mathbf{n}_b \, dl = \left(-\frac{\partial y_b}{\partial s} ds, \frac{\partial x_b}{\partial s} ds \right). \tag{27}$$

In the above equations, x_a, y_a, x_b and y_b are the interpolated coordinates on the boundaries of elements a and b, while $\mathbf{u}_a^A$ and $\mathbf{u}_b^A$ are the interpolated displacements corresponding to the displacement $\mathbf{U}_A$ at node A,

$$\mathbf{u}_a^A = \left(\frac{1+s}{2} - \frac{1-s^2}{2} \right) \mathbf{U}_A$$

$$\mathbf{u}_b^A = \left(\frac{1-s}{2} - \frac{1-s^2}{2} \right) \mathbf{U}_A. \tag{28}$$

For element a, mass conservation requires

$$\int_{L_a} \mathbf{u}_a^B \cdot \mathbf{n}_a \, dl = 0 \tag{29}$$

where $\mathbf{u}_a^B$ is the interpolated displacement on the boundary of element a based on the nodal displacement $\mathbf{U}_B$

$$\mathbf{u}_a^B = (1 - s^2)\mathbf{U}_B. \tag{30}$$

The relation (29) shows that the appropriate tangential direction β_B at node B is given by

$$\tan\beta_B = \frac{\partial y}{\partial s} \Big/ \frac{\partial x}{\partial s}\bigg|_B. \tag{31}$$

Our numerical experiments have shown that it is important to allocate the appropriate tangential directions at all boundary nodes. Otherwise spurious non-zero energy modes are obtained in the finite element solution.

6. NUMERICAL SOLUTIONS

To demonstrate the capability of the proposed formulation, we give the results obtained in the solution of three problems. We consider these analysis cases to be good tests because, while they pertain to simple problems, the degree of complexity seems to be sufficient to exhibit deficiencies in formulations. Until the development of the **u**–p–**A** formulation described here, we were not able to obtain accurate solutions to all these problems with a displacement-based formulation (or a formulation derived therefrom).

In all test problems, we want to evaluate the lowest frequencies of the coupled fluid–structure system. The problems were already considered by Olson and Bathe [4, 7].

Figure 4 describes the tilted piston-container problem. The massless elastic piston moves horizontally. Figure 5 describes the problem of a rigid cylinder vibrating in an acoustic cavity. The cylinder is sus-

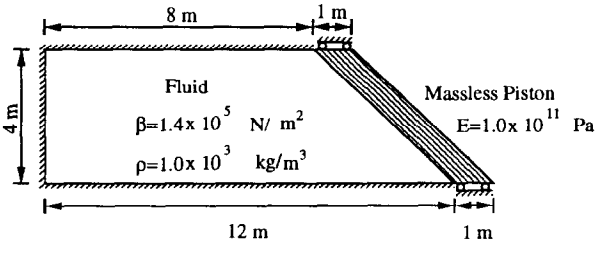

Fig. 4. Problem one: tilted piston-container system.

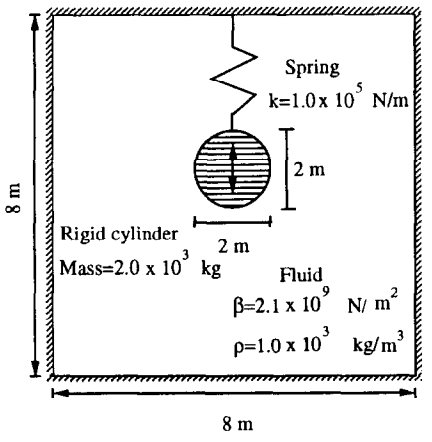

Fig. 5. Problem two: a rigid cylinder vibrating in an acoustic cavity.

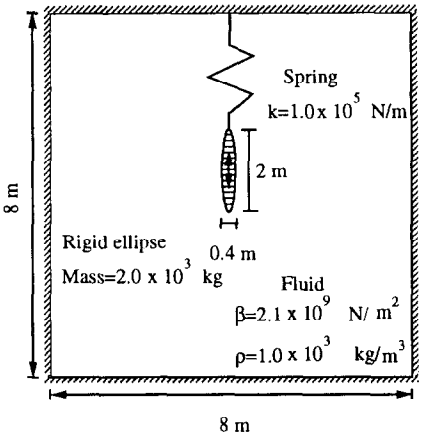

Fig. 6. Problem three: a rigid ellipse vibrating in an acoustic cavity.

pended from a spring and vibrates vertically in the fluid. Figure 6 shows a rigid ellipse on a spring in the same acoustic cavity. Figures 7–9 show typical nine-node element discretizations used in the analyses of the problems. Table 1 lists the results obtained using the 9-3-3 element, and Table 2 gives the results obtained with the velocity potential (that is $\mathbf{u}$–ϕ) formulation which can be considered a very reliable procedure [7]. The meshes used in these analyses have been derived by starting with coarse meshes and subdividing in each refinement each element into two or four elements. We also give in Table 1 the number

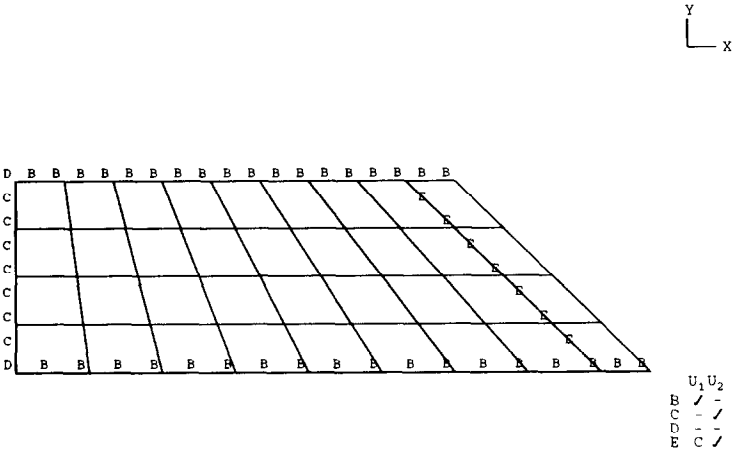

Fig. 7. Typical mesh for problem one.

Table 1. Analysis of test problems using 9-3-3 elements

Test case	Mesh, no. of elements	Number of zero frequencies		Frequencies (rad s^{-1})			
		Theory	Result	First	Second	Third	Fourth
Tilted	4	$\geqslant 7$	7	1.895	6.054	9.256	10.32
piston-	16	$\geqslant 31$	31	1.867	5.696	9.236	9.792
container	32	$\geqslant 63$	63	1.862	5.603	9.189	9.391
problem	64	$\geqslant 105$	105	1.859	5.589	8.617	9.175
Rigid	2	$\geqslant 1$	1	3.846	628.2	928.6	1341
cylinder	8	$\geqslant 13$	13	4.228	609.5	1191	1326
problem	32	$\geqslant 61$	61	4.281	589.4	1138	1252
	64	$\geqslant 125$	125	4.288	587.4	1131	1234
Rigid	2	$\geqslant 1$	1	5.511	629.9	932.6	1246
ellipse	8	$\geqslant 13$	13	6.612	589.1	1220	1232
problem	32	$\geqslant 61$	61	6.827	572.1	1155	1176
	64	$\geqslant 125$	125	6.829	571.2	1149	1167

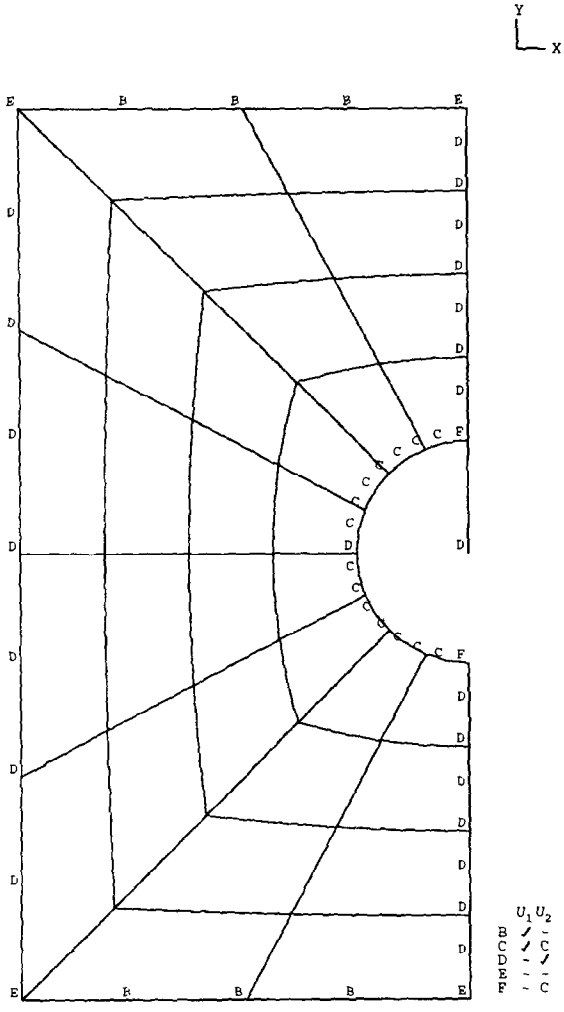

Fig. 8. Typical mesh for problem two.

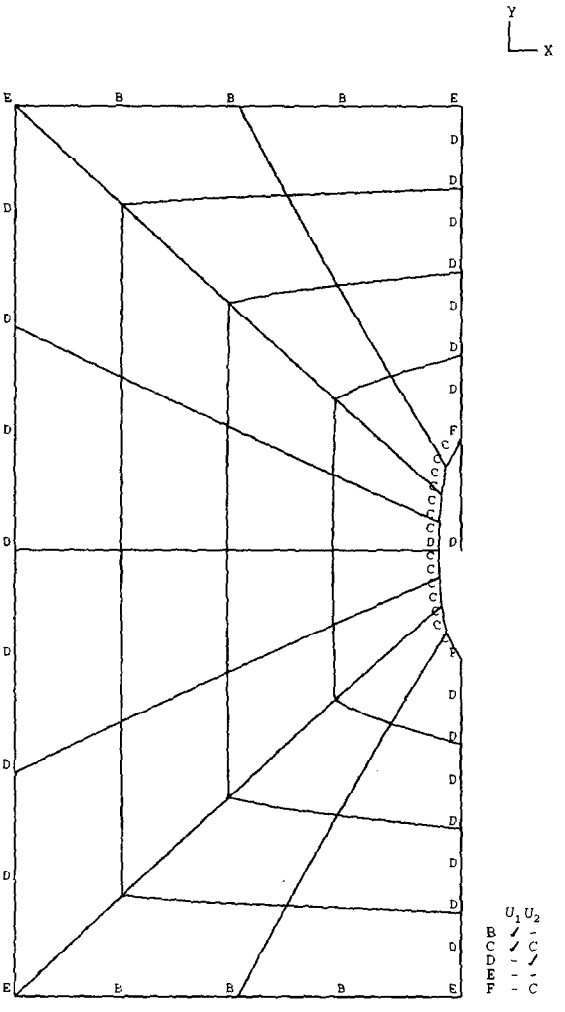

Fig. 9. Typical mesh for problem three.

of the zero frequencies k present in the analyses using the $\mathbf{u}$–p–Λ formulation. The theoretical result is obtained from the formula

$$k \geqslant nd - nc + 1 \tag{32}$$

where nd is the number of unconstrained displacement degrees of freedom in the model and nc is the sum of the pressure and vorticity moment degrees of freedom. Of course, we do not calculate the mode shapes corresponding to the zero frequencies, but simply shift to the non-zero frequencies sought [9].

The results in Tables 1 and 2 show that the $\mathbf{u}$–p–Λ formulation gives results close to those calculated with the $\mathbf{u}$–ϕ formulation, and that the number of zero frequencies matches the mathematical prediction. Figures 10–12 show pressure band plots of the modes considered in Table 1. The bands are quite smooth, indicating accurate solutions.

To illustrate the importance of assigning the appropriate tangential displacement directions at the fluid nodal points on the fluid–structure interfaces, we present the results of two test cases.

In the first test case, the very coarse finite element model shown in Fig. 13 for the response analysis of the rigid cylinder is considered. The assignment of the correct tangential directions at nodes 10 and 11 is critical. If we use the actual cylinder geometry, the

Table 2. Results obtained using $\mathbf{u}$–ϕ formulation for analysis of three test problems

Test case	Mesh, no. of elements	Frequencies (rad s^{-1}) First	Second	Third	Fourth
Tilted piston problem	32	1.858	5.569	9.116	9.299
Rigid cylinder problem	32	4.269	581.8	1124	1224
Rigid ellipse problem	32	7.071	563.2	1138	1158

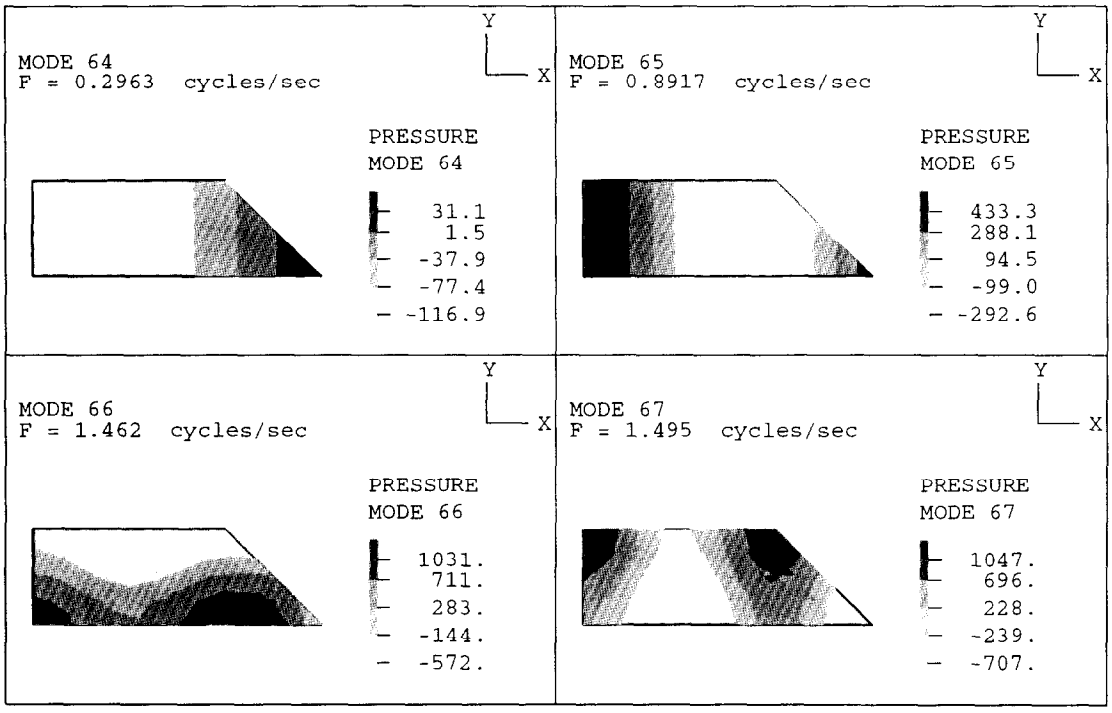

Fig. 10. Pressure bands of the first four modes of the tilted piston-container problem (mesh of 32 9-3-3 elements).

tangential directions are 60 and 120 degrees from the x-axis. However, using eqn (31) we obtain 45 and 135 degrees, respectively. Table 3 lists some solution results and shows that a spurious non-zero frequency appears when the incorrect tangential directions are assigned.

In the second test case, the finite element model shown in Fig. 14 is used for the frequency solution of the rigid ellipse vibrating in the fluid-filled cavity. If we use the tangential directions given by the actual geometry of the ellipse, a non-zero spurious frequency is calculated, whereas if the tangential directions are assigned using eqns (26) and (29), good solution results are obtained, see Table 3. The comparison of the angles (γ) from the x-axis obtained using eqns (26) and (29) with the angles using the actual geometry is as follows:

node 10: angle $\gamma|_{\text{model}} = 86.93°$
angle $\gamma|_{\text{geometry}} = 87.04°$

node 7: angle $\gamma|_{\text{model}} = 87.40°$
angle $\gamma|_{\text{geometry}} = 83.41°$

node 11: angle $\gamma|_{\text{model}} = 70.89°$
angle $\gamma|_{\text{geometry}} = 77.22°$.

It is interesting to note that based on the mass transport requirement the angle γ at node 7 is larger than at node 10, which is an unexpected result based on the actual geometry of the ellipse.

Finally, we also show results obtained with the 4-1-1 element. Since the 4/1 displacement/pressure element (that is, the element with four corner nodes for the displacement interpolation and a constant pressure assumption) for incompressible analysis does not satisfy the inf-sup condition, we expect that the 4-1-1 element will not provide a stable discretization. Table 4 and Figs 15 and 16 show some solution results. These clearly indicate that the 4-1-1 element is not a reliable element; the predicted lowest frequen-

Table 3. Spurious modes due to assignment of incorrect tangential displacement directions at the fluid–structure interfaces

Test case	Tangent direction	Number of zero frequencies		Frequencies (rad s^{-1})			
		Theory	Result	First	Second	Third	Fourth
Rigid cylinder model in Fig. 13	incorrect	≥ 5	4	4.649	86.17	693.7	1154
	correct	≥ 5	5	3.861	688.2	1169	1324
Rigid ellipse model in Fig. 14	incorrect	≥ 13	12	6.719	34.65	591.4	1213
	correct	≥ 13	13	6.612	589.1	1220	1232

Table 4. Solution results using 4-1-1 elements

Test case	Mesh, no. of elements	Frequencies (rad s^{-1}) First	Second	Third	Fourth
Rigid cylinder problem	128	11.91	581.8	1135	1234
Rigid ellipse problem	128	557.5	988.2	1157	1180

cies are not accurate and the checkerboard pressure bands obtained here are typical of those observed with the 4/1 element in incompressible analysis.

7. CONCLUSIONS

A new effective three-field mixed finite element formulation for analysis of acoustic fluids and their interactions with structures has been presented. The fluid formulation has the following attributes:

(1) The displacement, pressure and vorticity moment are used as independent variables. For the element interpolations it is effective that the pressure and vorticity moment are associated with element internal variables and are statically condensed out at the element level. Then the only nodal point variables used in the assemblage of elements are those corresponding to the displacements. This enables the direct coupling of the fluid elements with the structural elements. Of course, in principle, we could also employ element nodal pressures and vorticity moments that provide for continuity in these variables (and hence cannot be statically condensed out at the element level).

(2) The key point is to choose the appropriate interpolations for the displacements, pressure and

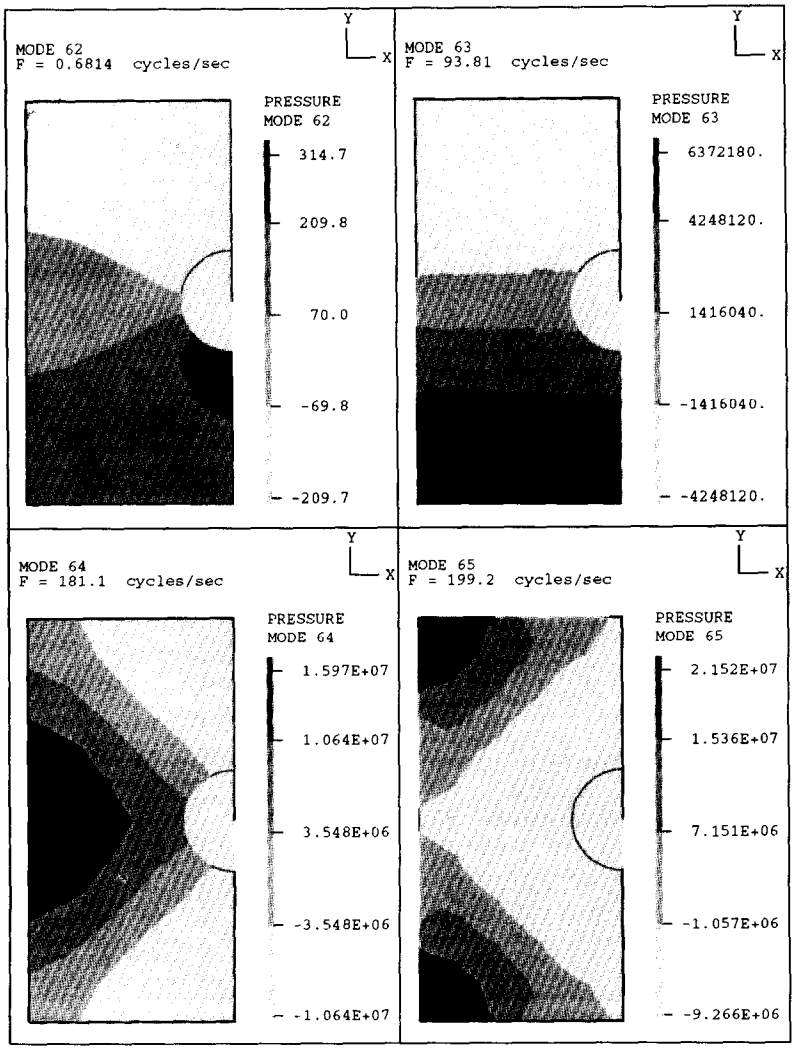

Fig. 11. Pressure bands of the first four modes of the rigid cylinder problem (mesh of 32 9-3-3 elements).

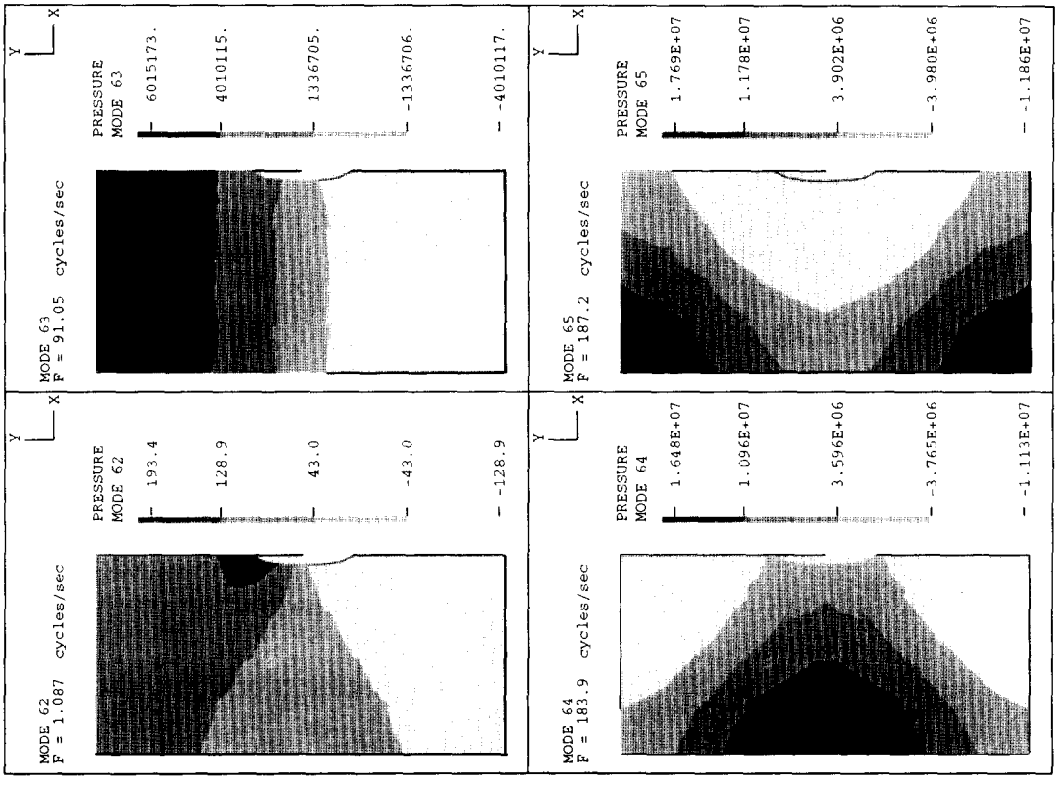

Fig. 12. Pressure bands of the first four modes of the rigid ellipse problem (mesh of 32 9-3-3 elements).

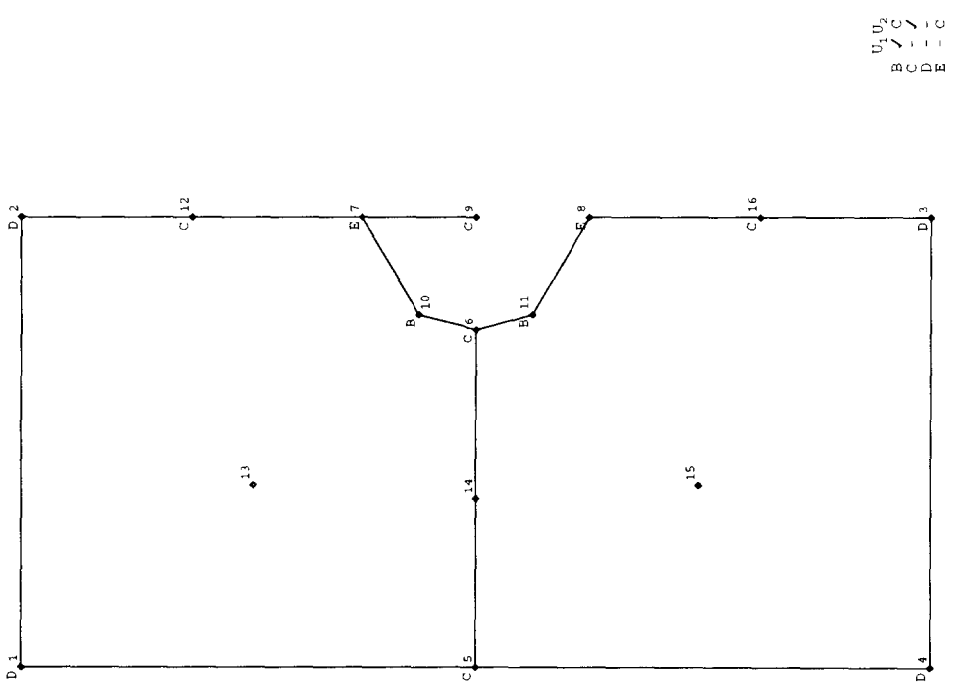

Fig. 13. Response analysis of rigid cylinder; use of two 9-3-1 elements.

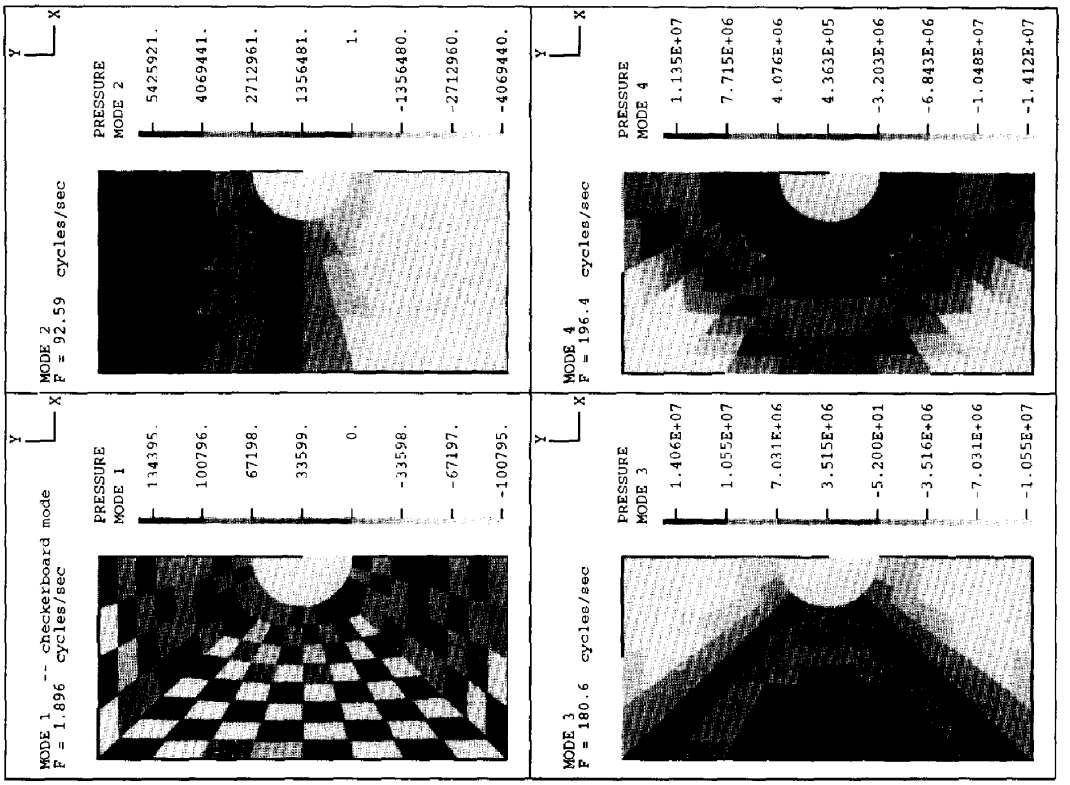

Fig. 15. Checkerboard pressure band of problem two with 4-1-1 elements.

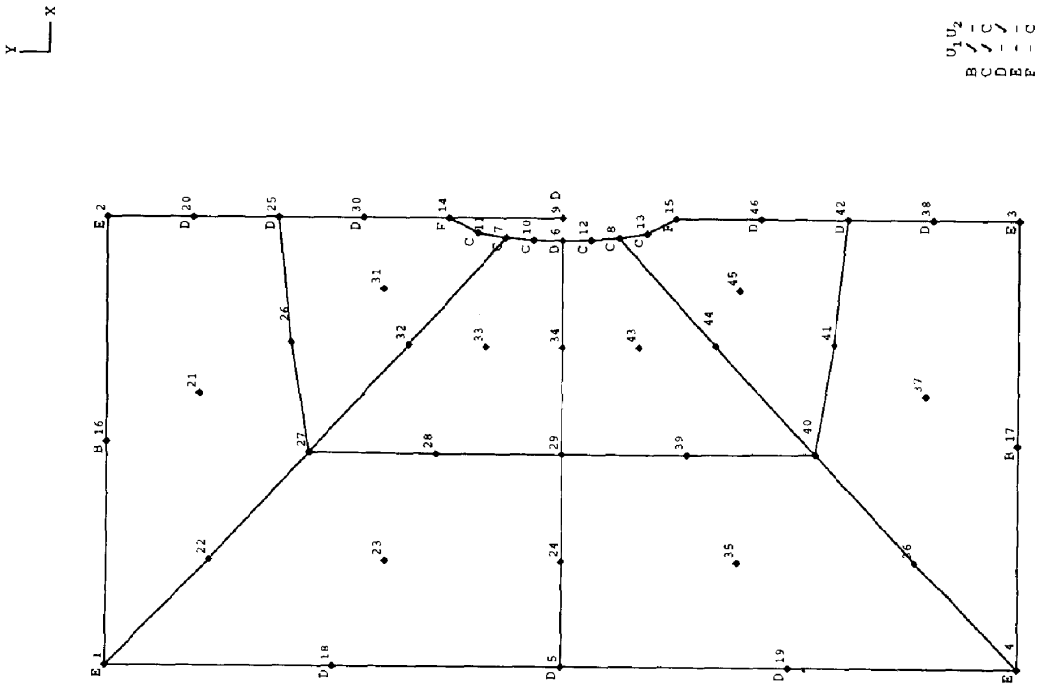

Fig. 14. Response analysis of rigid ellipse; use of eight 9-3-3 elements.

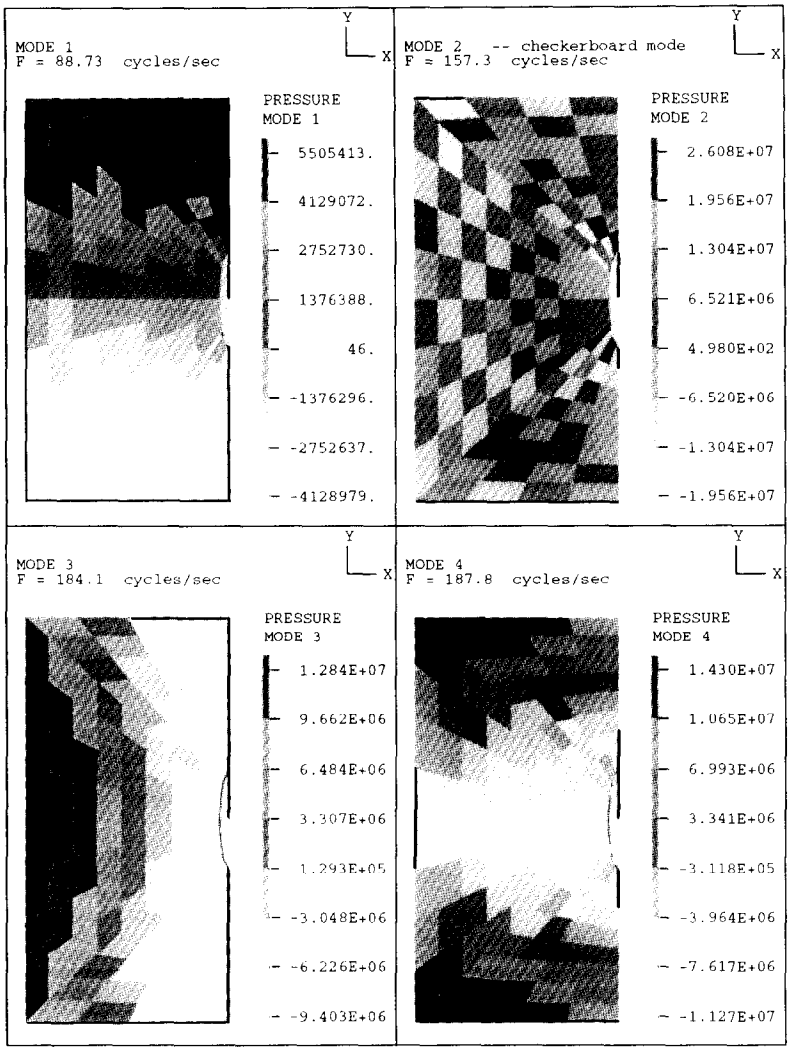

Fig. 16. Checkerboard pressure band of problem three with 4-1-1 elements.

vorticity moment. We employ the same interpolations as used for stable discretizations in the displacement (or velocity)/pressure formulations of almost incompressible media. We have no mathematical proof that the inf-sup condition is satisfied using these interpolations, but believe that our interpolations are reasonable because the constraints of pressure and vorticity moment are imposed independently in the formulation.

(3) Specific attention need be given to the evaluation of the tangential (slip) directions at the fluid solid interfaces. These directions need to satisfy relations of mass conservation.

(4) We have tested the formulation on some simple but well-chosen analysis problems, which heretofore we could not solve with displacement-based finite element formulations (or formulations derived therefrom). The new formulation has performed well in all analysis cases. The results of some numerical experiments on the use of a four-node element which is not recommended for general use and inappropriate boundary tangential directions have been included in order to illustrate the importance of our recommendations.

While the formulation presented here shows much promise, we are continuing our work on the topic of this paper because we expect that an even simpler and more effective mixed displacement-based finite element formulation can be reached.

Acknowledgement—We would like to thank F. Brezzi, University of Pavia, Italy, for our discussions on this research.

REFERENCES

1. M. A. Hamdi, Y. Ousset, and G. Verchery, A displacement method for the analysis of vibrations of coupled fluid–structure systems. *Int. J. numer. Meth. Engng* **13**, 139–150 (1978).
2. T. B. Belytschko and J. M. Kennedy, A fluid–structure finite element method for the analysis of reactor safety problems. *Nucl. Engng Des.* **38**, 71–81 (1976).
3. T. Belytschko, Fluid–structure interaction. *Comput. Struct.* **12**, 459–469 (1980).

4. L. G. Olson and K. J. Bathe, A study of displacement-based fluid finite elements for calculating frequencies of fluid and fluid–structure systems. *Nucl. Engng Des.* **76,** 137–151 (1983).
5. H. Morand and R. Ohayon, Substructure variational analysis of the vibrations of coupled fluid–structure systems. Finite element results. *Int. J. numer. Meth. Engng* **14,** 741–755 (1979).
6. G. C. Everstine, A symmetric potential formulation for fluid–structure interaction. *J. Sound Vibr.* **79**(1), 157–160 (1981).
7. L. G. Olson and K. J. Bathe, Analysis of fluid–structure interactions. A direct symmetric coupled formulation based on the fluid velocity potential. *Comput. Struct.* **21**(1,2), 21–32 (1985).
8. H. C. Chen and R. L. Taylor, Vibration analysis of fluid-solid systems using a finite element displacement formulation. *Int. J. numer. Meth. Engng* **29,** 683–698 (1990).
9. K. J. Bathe, *Finite Element Procedures.* Prentice Hall, Englewood Cliffs, NJ (1995).
10. F. Brezzi and M. Fortin, *Mixed and Hybrid Finite Element Methods.* Springer, Berlin (1991).
11. D. Chapelle and K. J. Bathe, The inf-sup test. *Comput. Struct.* **47**(4,5), 537–545 (1993).
12. K. J. Bathe, J. Walczak, and H. Zhang, Some recent advances for practical finite element analysis. *Comput. Struct.* **47**(4,5), 511–521 (1993).
13. J. Donea, S. Giuliani, and J. P. Halleux, An arbitrary Lagrangian–Eulerian finite element method for transient dynamic fluid–structure interactions. *Comput. Meth. appl. mech. Engng* **33,** 689–723 (1982).